CHEMISTRY OF MATERIALS
Article

Chem. Mater. **2009,** *21,* 5413–5425 5413
DOI:10.1021/cm901999n

New Understanding and Simple Approach to Synthesize Highly Hydrothermally Stable and Ordered Mesoporous Materials

Dahai Pan,[†] Pei Yuan,[‡] Linzhi Zhao,[‡] Nian Liu,[‡] Liang Zhou,[‡] Guangfeng Wei,[‡] Jun Zhang,[‡] Yichuan Ling,[‡] Yu Fan,[†] Baoying Wei,[†] Haiyan Liu,[†] Chengzhong Yu,*[,‡] and Xiaojun Bao*[,†]

[†]*State Key Laboratory of Heavy Oil Processing, China University of Petroleum, No. 18 Fuxue Road, Changping, Beijing 102249, PR China, and* [‡]*Department of Chemistry and Shanghai Key Laboratory of Molecular Catalysis and Innovative Materials, Fudan University, Shanghai, 200433, PR China*

Received July 5, 2009. Revised Manuscript Received August 23, 2009

Highly ordered mesoporous materials with extremely high hydrothermal stability have been successfully synthesized by a novel and facile approach. Our method is built on the understanding that the hydrothermal treatment process plays an important role in the synthesis of mesoporous materials. It is proposed that in order to use high temperature hydrothermal treatment to increase the inorganic framework cross-linkage, an important requirement is that the organic surfactants must be retained as much as possible to maintain the preformed organic−inorganic composite mesostructure against framework shrinkage during the hydrothermal treatment process. This requirement can be achieved by enhancing the surfactant−silanol interaction at the organic−inorganic interface through adjusting the hydrothermal treatment pH and adding acetic acid (HAc) during the synthesis. When a high temperature (∼200 °C) hydrothermal treatment is employed, ordered mesoporous materials can only be obtained in a hydrothermal treatment pH range of 1−3. When the hydrothermal treatment pH is near the isoelectric point of silica, the highest silanol density on silica walls can entrap the largest amount of surfactants within pores, resulting in highly ordered mesostructured materials. Moreover, the disadvantage of the hydrothermal treatment under strong acidic conditions widely adopted in the literature has been revealed. Compared to previous reports, our approach is simple and does not involve environmentally unfriendly or expensive agents, thus is easy to be scaled up for industrial applications. Most strikingly, the highly ordered mesostructure of aluminosilicate synthesized by our approach can be maintained after steam treatment at 800 °C for 5 h with only a 4.9% decrease in the Brunauer−Emmett−Teller surface area. Our achievements have added new contributions to understanding the preparation of highly ordered and highly stable mesoporous materials, which sheds light on the practical applications of this new family of porous materials in the petroleum and petrochemical industry.

Introduction

Since their first invention in 1992,[1,2] ordered mesoporous materials with tunable structures, high surface areas and pore volumes have attracted extensive attention for their potential applications as advanced catalysts, adsorbents, optical guides, and sensors, etc.[3−13] Compared to zeolites generally with micropores, mesoporous materials with large, uniform, and adjustable pore size are advantageous for catalytic reactions in the petrochemical industry, especially for the conversion of heavy oil molecules.[3,7,12] For applications that require long-lasting exposure of mesoporous materials to hydrothermal environments (such as catalytic cracking of heavy oil), the stability of mesoporous materials is very important, which remains to be a great challenge that severely hinders the practical applications of mesoporous materials.

*Corresponding authors. E-mail: czyu@fudan.edu.cn (C.Y.); baoxj@cup.edu.cn (X.B.).

(1) Kresge, C. T.; Leonowicz, M. E.; Roth, W. J.; Vartuli, J. C.; Beck, J. S. *Nature* **1992**, *359*, 710.
(2) Beck, J. S.; Vartuli, J. C.; Roth, W. J.; Leonowicz, M. E.; Kresge, C. T.; Schmitt, K. D.; Chu, C. T. W.; Olson, D. H.; Sheppard, E. W.; McCullen, S. B.; Higgins, J. B.; Schlenker, J. L. *J. Am. Chem. Soc.* **1992**, *114*, 10834.
(3) Corma, A. *Chem. Rev.* **1997**, *97*, 2373.
(4) Sayari, A. *Chem. Mater.* **1996**, *8*, 1840.
(5) Ariga, K.; Vinu, A.; Hill, J. P.; Mori, T. *Coord. Chem. Rev.* **2007**, *251*, 2562.
(6) Kuchibhatla, S.; Karakoti, A. S.; Bera, D.; Seal, S. *Prog. Mater. Sci.* **2007**, *52*, 699.
(7) On, D. T.; Desplantier-Giscard, D.; Danumah, C.; Kaliaguine, S. *Appl. Catal. A-Gen.* **2001**, *222*, 299.
(8) Srivastava, R.; Choi, M.; Ryoo, R. *Chem. Commun.* **2006**, 4489.
(9) Wan, Y.; Shi, Y. F.; Zhao, D. Y. *Chem. Commun.* **2007**, 897.
(10) Tao, Y. S.; Kanoh, H.; Abrams, L.; Kaneko, K. *Chem. Rev.* **2006**, *106*, 896.
(11) Wan, Y.; Zhao, D. Y. *Chem. Rev.* **2007**, *107*, 2821.
(12) Taguchi, A.; Schuth, F. *Microporous Mesoporous Mater.* **2005**, *77*, 1.
(13) Davis, M. E. *Nature* **2002**, *417*, 813.

Published on Web 10/27/2009

Great efforts have been devoted to increase the hydrothermal stability of mesoporous materials.[14−47] For examples, mesoporous materials with thick pore walls have been prepared using triblock copolymers as templates.[14,15] Vesiclelike Michigan State University Material (MSU-G) materials with a high framework cross-linkage have been obtained templated with neutral gemini surfactants.[16] The use of inorganic salts can also increase the stability of materials.[17−21] Through the incorporation of heteroatoms by direct synthesis[22−25] or post-treatment grafting procedures,[26−31] stable mesoporous aluminosilicates have been obtained. In addition, postsynthesis treatment[32] or thermal treatment at high temperature[33] can enhance the polymerization degree of ≡Si—O—Si≡ bonds and effectively improve the hydrothermal stability of resultant mesoporous materials. Although most of these materials exhibited high hydrothermal stability in boiling water, few retained well-ordered mesostructure after being treated in steam at high temperature (e.g., 800 °C), which is a requisite process for many important petrochemical processes.

Another approach to increase the hydrothermal stability of mesoporous materials is to synthesize mesoporous aluminosilicates with improved framework crystallinity. In some cases, molecular templates for zeolites were added in the synthesis of mesoporous aluminosilicates in order to achieve both mesostructure assembly and zeolite crystallization in mesopore walls concurrently.[34−36] However, such a protocol frequently produces amorphous mesoporous materials, bulk zeolite crsytals without mesoporosity, or their physical mixtures, because the molecular crystallization and supramolecular self-assembly processes generally proceed in a competitive manner.[44,48,49] By using preformed zeolite nanoclusters or zeolite seeds that consist of primary or secondary building units as precursors to self-assemble with surfactant templates, the problem of zeolite phase-separation from mesophase can be solved, thus mesoporous aluminosilicates and titanium silicates with highly hydrothermal stability have been synthesized in strong acidic media.[37−43] For the products prepared via such a route, their acidity and hydrothermal stability were improved to a certain extent; however, their properties were still far from those of crystalline zeolites.[50] In addition, this synthesis strategy involves multisteps and is relatively complex. Recently, it was also reported that mesoporous materials with crystalline zeolite framework can be synthesized directly by using amphiphilic organosilanes as a mesopore-directing agent.[44] In addition, Fan and co-workers have synthesized larger zeolite particles with three-dimensionally ordered mesopores by using three-dimensionally ordered mesoporous carbon as a template.[45] Nevertheless, unusual and expensive templates were used in the above two reports, which are not economical for industrial scale production.

Increasing silica wall thickness and enhancing wall cross-linkage are two effective methods to increase the hydrothermal stability of mesoporous materials. Compared to MCM-41S materials,[1,2] SBA-15 type materials with larger pore diameters and thicker pore walls show relatively higher hydrothermal stability and great advantages in potential applications.[14,15] However, the hydrothermal stability of original SBA-15 in steam at 800 °C is far from satisfactory. To further enhance the silica condensation in mesoporous walls, increasing the hydrothermal treatment temperatures should be a simple and effective strategy. However, it is generally accepted that the decomposition of block copolymer templates occurs at high temperatures, which requires that the hydrothermal treatment temperature should be lower than 160 °C in the absence of other additives. By further introducing

(14) Zhao, D. Y.; Feng, J. L.; Huo, Q. S.; Melosh, N.; Fredrickson, G. H.; Chmelka, B. F.; Stucky, G. D. *Science* **1998**, *279*, 548.
(15) Zhao, D. Y.; Huo, Q. S.; Feng, J. L.; Chmelka, B. F.; Stucky, G. D. *J. Am. Chem. Soc.* **1998**, *120*, 6024.
(16) Kim, S. S.; Zhang, W. Z.; Pinnavaia, T. J. *Science* **1998**, *282*, 1302.
(17) Ryoo, R.; Jun, S. *J. Phys. Chem. B* **1997**, *101*, 317.
(18) Kim, J. M.; Jun, S.; Ryoo, R. *J. Phys. Chem. B* **1999**, *103*, 6200.
(19) Das, D.; Tsai, C. M.; Cheng, S. F. *Chem. Commun.* **1999**, 473.
(20) Li, C. L.; Wang, Y. Q.; Guo, Y. L.; Liu, X. H.; Guo, Y.; Zhang, Z. G.; Wang, Y. S.; Lu, G. Z. *Chem. Mater.* **2007**, *19*, 173.
(21) Du, Y. C.; Lan, X. J.; Liu, S.; Ji, Y. Y.; Zhang, Y. L.; Zhang, W. P.; Xiao, F. S. *Microporous Mesoporous Mat.* **2008**, *112*, 225.
(22) Xia, Y. D.; Mokaya, R. *J. Phys. Chem. B* **2003**, *107*, 6954.
(23) Yang, Q. H.; Li, Y.; Zhang, L.; Yang, J.; Liu, J.; Li, C. *J. Phys. Chem. B* **2004**, *108*, 7934.
(24) Shen, S. C.; Kawi, S. *J. Phys. Chem. B* **1999**, *103*, 8870.
(25) Mokaya, R. *J. Phys. Chem. B* **2000**, *104*, 8279.
(26) Mokaya, R.; Jones, W. *Chem. Commun.* **1998**, 1839.
(27) Mokaya, R. *Angew. Chem.-Int. Ed.* **1999**, *38*, 2930.
(28) Yang, X. Y.; Vantomme, A.; Lemaire, A.; Xiao, F. S.; Su, B. L. *Adv. Mater.* **2006**, *18*, 2117.
(29) Wu, P.; Tatsumi, T.; Komatsu, T.; Yashima, T. *Chem. Mater.* **2002**, *14*, 1657.
(30) Shen, S. C.; Kawi, S. *Langmuir* **2002**, *18*, 4720.
(31) Wang, K. X.; Lin, Y. J.; Morris, M. A.; Holmes, J. D. *J. Mater. Chem.* **2006**, *16*, 4051.
(32) Galarneau, A.; Driole, M. F.; Petitto, C.; Chiche, B.; Bonelli, B.; Armandi, M.; Onida, B.; Garrone, E.; di Renzo, F.; Fajula, F. *Microporous Mesoporous Mater.* **2005**, *83*, 172.
(33) Zhang, F. Q.; Yan, Y.; Yang, H. F.; Meng, Y.; Yu, C. Z.; Tu, B.; Zhao, D. Y. *J. Phys. Chem. B* **2005**, *109*, 8723.
(34) Beck, J. S.; Vartuli, J. C.; Kennedy, G. J.; Kresge, C. T.; Roth, W. J.; Schramm, S. E. *Chem. Mater.* **1994**, *6*, 1816.
(35) Karlsson, A.; Stocker, M.; Schmidt, R. *Microporous Mesoporous Mater.* **1999**, *27*, 181.
(36) Petkov, N.; Holzl, M.; Metzger, T. H.; Mintova, S.; Bein, T. *J. Phys. Chem. B* **2005**, *109*, 4485.
(37) Liu, Y.; Zhang, W. Z.; Pinnavaia, T. J. *Angew. Chem.-Int. Ed.* **2001**, *40*, 1255.
(38) Liu, Y.; Zhang, W. Z.; Pinnavaia, T. J. *J. Am. Chem. Soc.* **2000**, *122*, 8791.
(39) Wang, H.; Liu, Y.; Pinnavaia, T. J. *J. Phys. Chem. B* **2006**, *110*, 4524.
(40) Zhang, Z. T.; Han, Y.; Zhu, L.; Wang, R. W.; Yu, Y.; Qiu, S. L.; Zhao, D. Y.; Xiao, F. S. *Angew. Chem.-Int. Ed.* **2001**, *40*, 1258.
(41) Zhang, Z. T.; Han, Y.; Xiao, F. S.; Qiu, S. L.; Zhu, L.; Wang, R. W.; Yu, Y.; Zhang, Z.; Zou, B. S.; Wang, Y. Q.; Sun, H. P.; Zhao, D. Y.; Wei, Y. *J. Am. Chem. Soc.* **2001**, *123*, 5014.
(42) Zhang, Z.; Han, Y.; Zhu, L.; Wang, R.; Yu, Y.; Qiu, S.; Zhao, D.; Xiao, F. S. *Angew. Chem.-Int. Ed.* **2002**, *41*, 2226.
(43) Han, Y.; Li, N.; Zhao, L.; Li, D. F.; Xu, X. Z.; Wu, S.; Di, Y.; Li, C. J.; Zou, Y. C.; Yu, Y.; Xiao, F. S. *J. Phys. Chem. B* **2003**, *107*, 7551.
(44) Choi, M.; Cho, H. S.; Srivastava, R.; Venkatesan, C.; Choi, D. H.; Ryoo, R. *Nat. Mater.* **2006**, *5*, 718.
(45) Fan, W.; Snyder, M. A.; Kumar, S.; Lee, P.-S.; Yoo, W. C.; Mccormick, A. V.; Penn, R. L.; Stein, A.; Tsapatsis, M. *Nat. Mater.* **2008**, *7*, 984.
(46) Han, Y.; Li, D. F.; Zhao, L.; Song, J. W.; Yang, X. Y.; Li, N.; Di, Y.; Li, C. J.; Wu, S.; Xu, X. Z.; Meng, X. J.; Lin, K. F.; Xiao, F. S. *Angew. Chem.-Int. Ed.* **2003**, *42*, 3633.
(47) Li, D. F.; Han, Y.; Song, H. W.; Zhao, L.; Xu, X. Z.; Di, Y.; Xiao, F. S. *Chem.—Eur. J.* **2004**, *10*, 5911.
(48) Christiansen, S. C.; Zhao, D. Y.; Janicke, M. T.; Landry, C. C.; Stucky, G. D.; Chmelka, B. F. *J. Am. Chem. Soc.* **2001**, *123*, 4519.
(49) Hedin, N.; Graf, R.; Christiansen, S. C.; Gervais, C.; Hayward, R. C.; Eckert, J.; Chmelka, B. F. *J. Am. Chem. Soc.* **2004**, *126*, 9425.
(50) Xia, Y. D.; Mokaya, R. *J. Mater. Chem.* **2004**, *14*, 3427.

special surfactants such as high-temperature stable fluorocarbon surfactants as templates or additives, a series of ordered mesoporous silica-based materials with a high degree of silica condensation have been synthesized at temperatures ranging from 160 to 190 °C.[20,46,47] However, the use of environmentally unfriendly and very expensive fluorocarbon surfactants may severely hinder the practical application of this route. Therefore, finding a facile, environmentally benign, and cost-effective synthesis of highly ordered mesoporous materials with high hydrothermal stability still poses a challenge.

With the understanding that the hydrothermal treatment is a necessary step in the synthesis of SBA-15 type materials[9,11] and increasing the hydrothermal treatment temperature can increase the hydrothermal stability, it is surprising to find out that in the previous literature little has been done to understand at the molecular or supramolecular level what happens during the hydrothermal treatment process. For example, the hydrothermal treatment is generally carried out under a strong acidic condition (in a 2.0 M HCl solution) following the original report,[14,15] but it is not clear why ordered mesostructures cannot be maintained when the hydrothermal treatment temperature exceeds 160 °C in the absence of additives and how to overcome this limit. A systematical study of the influence of hydrothermal treatment pH and temperature on the mesostructural regularity and stability will be important to design and synthesize highly ordered and highly stable mesoporous materials.

Herein, we report a novel and facile approach to synthesize highly ordered and highly hydrothermally stable mesoporous materials. Our approach is designed based on a new understanding and aiming at future large scale synthesis. To synthesize highly ordered and highly stable mesoporous materials, we focus on the hydrothermal treatment process. We propose that in order to fully take the advantage of high temperature hydrothermal treatment to increase the inorganic framework cross-linkage, the most important issue is to retain organic surfactants as much as possible to maintain the preformed organic−inorganic composite mesostructure against framework shrinkage. This can be achieved by enhancing the surfactant−silanol interaction at the organic−inorganic interface through adjusting the hydrothermal treatment pH and by adding acetic acid (HAc) during the synthesis. Moreover, the disadvantage of hydrothermal treatment process under strong acidic condition widely adopted in the literature has been revealed for the first time. Compared to previous reports, our approach is simple and does not involve environmentally unfriendly or expensive agents, which is easy to be scaled up for industrial applications. Most strikingly, the highly ordered mesostructure of aluminosilicate synthesized by our approach can be maintained after steam treatment at 800 °C for 5 h with only a 4.9% decrease in the Brunauer−Emmett−Teller (BET) surface area. Our achievements have added new contributions to understanding the preparation of highly ordered and highly stable mesoporous materials, which sheds light on the practical applications of this new family of porous materials.

Experimental Section

Materials. Triblock copolymer P123 (M_w = 5800, $EO_{20}PO_{70}EO_{20}$) was purchased from Aldrich. Tetraethyl orthosilicate (TEOS), aluminum iso-propoxide, hydrochloric acid (HCl), and acetic acid (HAc) were obtained from Shanghai Chemical Co., P.R. China. All of the chemicals were used as received without further purification.

Synthesis of Silica Mesoporous Materials. A typical synthesis is described as follows. A 1 g portion of P123 and a required amount of HAc were dissolved in 30 mL of 2.0 M HCl aqueous solution, followed by the addition of 2.08 g of TEOS under stirring. After being stirred at 38 °C for 24 h, the resulting white precipitate was filtrated and washed for three times. The product was mixed with 20 g of deionized water, and the pH value of the solution was adjusted from 0.16 to 4.66 using 2.0 M HCl. The mixture was transferred into an autoclave for hydrothermal treatment at a given temperature (adjusted from 100 to 220 °C) for 24 h. The final as-synthesized product was collected by filtration, washed with deionized water, and dried in air.

Compared with the original synthesis method of SBA-15,[14,15] our approach has the following three main changes: (1) the adjustment of pH during the hydrothermal treatment process, (2) the addition of HAc, and (3) the variation of the hydrothermal treatment temperature. Thus the samples synthesized under different conditions were named as S-*X*-*Y*-*T*, where S is the abbreviation of a sample, *X* denotes the pH value of the hydrothermal treatment solution, *Y* stands for the molar ratio of HAc to P123 (n_{HAc}/n_{P123}), and *T* denotes the hydrothermal treatment temperature. For instance, S-1.65-150-200 refers to the sample prepared with the pH value and the molar ratio of HAc/P123 at 1.65 and 150, respectively, and the hydrothermal treatment temperature is 200 °C. In addition, SBA-15 prepared by the traditional method reported by Zhao[14,15] (prepared and hydrothermally treated in 2.0 M hydrochloric acid solution) were designated as S-2M-*Y*-*T*.

All samples were calcined at 650 °C for 5 h to remove the surfactants. For selected samples, the block copolymers were extracted from the as-synthesized samples by a mixture of 80 mL of ethanol and 2.4 g of concentrated HCl at 60 °C three times (stirring for 8 h each time).

Synthesis of Mesoporous Aluminosilicate Material Al/S-1.65-150-200. A 0.070 g portion of aluminum iso-propoxide and 2.08 g of TEOS were simultaneously dissolved in 30 mL of 2.0 M HCl aqueous solution containing 1 g of P123 and 1.55 g of HAc. The followed steps were the same as those described in the synthesis of silica sample S-1.65-150-200.

P123 Adsorption. The surfactant inside the mesopores of the sample S-2M-0-100 was removed by calcination and extraction, respectively. Then 0.6 g of calcined S-2M-0-100 and extracted S-2M-0-100 were separately added into a 30 mL aqueous solution containing 1 g of P123, stirred at room temperature for 24 h, and collected by filtration. The adsorbed P123 amount was calculated from the mass loss after the complete removal of physisorbed water by thermogravimetry analysis (TGA). For reference, the mass loss of water during further condensation of silanols and partially retained P123 in extracted S-2M-0-100 was also measured by TGA.

Hydrothermal Stability Evaluation. The hydrothermal stability was investigated by treating calcined samples in a

closed bottle at 100 °C for 168 h under static conditions. The high-temperature hydrothermal stability of calcined samples was tested by treating samples at 800 °C for 2 and 5 h in 15% steam in nitrogen atmosphere, and the flow rate of nitrogen was 45 mL/min.

Characterization. X-ray diffraction (XRD) patterns were obtained on a Bruker D4 powder X-ray diffractometer using Ni-filtered Cu Kα radiation. Transmission electron microscopy (TEM) experiments were performed on a JEOL 2011 microscope operated at 200 kV. Nitrogen adsorption−desorption isotherms were measured on a Quantachrome analyzer at −196 °C. Before measurements, the samples were degassed at 180 °C in vacuum for 10 h. The BET method was used to calculate the specific surface areas. The pore volume and pore size distributions were derived from the adsorption branches of the isotherms using the Barrett−Joyner−Halenda (BJH) method. The total pore volume, V_p, was calculated from the nitrogen amount adsorbed at a relative pressure of 0.99. ^{29}Si solid-state nuclear magnetic resonance (NMR) single pulse experiments with proton decoupling were performed on a Bruker DSX300 spectrometer operated at a frequency of 59.63 MHz, a relaxation time of 600 s, a pulse-width of 4.8 us, a radiation frequency intensity of 62.5 kHz, and with $[(CH_3)_3SiO]_8Si_8O_{12}$ (Q_8M_8) as reference. The data collection time is ~18 h per sample. The TGA profiles were carried out between 25 and 600 °C in air using a Mettler Toledo TGA/SDTA 851e instrument. The air flow rate was 80 mL/min, and the heating rate was 2 °C/min. The in situ Fourier transform infrared (FTIR) spectra were collected with a Nicolet Nexus 470 FTIR spectrometer. For each spectrum, 64 scans were collected at a resolution of 4 cm^{-1} over the range of 400−4000 cm^{-1}. Before analysis, the surfactant-extracted samples were pressed into wafers with the same weight and area and, then, mounted onto a high-vacuum cell equipped with calcium fluoride windows. The samples were dehydrated in high-vacuum (10^{-6} Pa) at 120 °C for 4 h. The concentration of silanol (Si−OH) groups was measured from the integral area of the Si−OH absorbent peak after the complete removal of physisorbed water. The Si−OH density was calculated from the ratio of the concentration of Si−OH groups over the specific surface area (S_{BET}). In addition, the Si−OH density of surfactant extracted sample S-1.26-150-200 was considered to be 100% as a benchmark, and the relative silanol density was calculated by the following equation:

$$\text{relative silanol density} = \frac{\text{silanol density of other extracted sample}}{\text{silanol density of extracted S-1.26-150-200}} \times 100\%$$

Results and Discussion

Synthesis, Characterization, and Mechanism Study. The powder XRD patterns of the calcined mesoporous materials prepared with the different methods and hydrothermally treated at 200 °C are shown in Figure 1. Samples S-1.65-150-200 and S-1.65-0-200 prepared at a hydrothermal treatment pH of 1.65 exhibit three well-resolved Bragg peaks, indicating a highly ordered mesostructure even after a high temperature hydrothermal treatment. For calcined S-1.65-150-200, three diffraction peaks are observed at $2\theta = 0.98$, 1.69, and 1.92° with a reciprocal d-spacing ratio close to $1:\sqrt{3}:2$, which can be indexed as the (100), (110), and (200) reflections of a 2D hexagonal

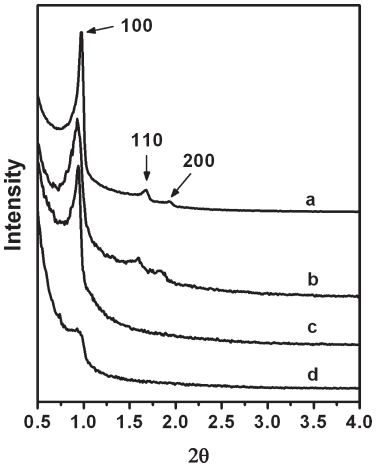

Figure 1. XRD patterns of the calcined materials synthesized at different conditions: (a) S-1.65-150-200, (b) S-1.65-0-200, (c) S-2M-150-200, and (d) S-2M-0-200.

Table 1. Physicochemical Properties of Calcined Samples Prepared at Different Conditions[a]

sample	a (nm)	D_p (nm)	S_{BET} (m^2/g)	V_p (cm^3/g)	φ (%)
S-1.65-150-200	10.4	11.2	367	0.91	35.1
S-1.65-0-200	11.0	18.1	280	0.87	21.9
S-2M-150-200	11.1		230	0.97	6.6
S-2M-0-200	10.7		143	0.11	2.2

[a] a = cell dimension; D_p = pore diameter; V_p = total pore volume; φ = mass loss (%). Because S-2M-150-200 and S-2M-0-200 were rendered disordered after the hydrothermal treatment at 200 °C, there was no pore sizes for the calcined samples given in this table.

mesostructure (space group *p6mm*). From the intense (100) peak, a d_{100} spacing of 9.0 nm is calculated, corresponding to a unit cell parameter (a) of 10.4 nm (Table 1). Compared to the XRD pattern of calcined S-1.65-150-200 (Figure 1a), calcined S-1.65-0-200 prepared without the addition of HAc exhibits relatively lower signal-to-noise ratio in its XRD pattern (Figure 1b) and broader full width at half-maximum (fwhm) as judged from the (100) diffraction peak (from 0.13 to 0.27°), suggesting that the ordering of the mesostructure decreases to a certain degree. For calcined S-2M-150-200 and S-2M-0-200 prepared with a hydrothermal treatment performed under a very acidic condition (2.0 M HCl), only one peak is observed, showing the crucial role of the hydrothermal treatment pH for synthesizing highly ordered mesostructures in a high temperature hydrothermal treatment process. In addition, compared to that of calcined S-2M-0-200, the XRD pattern of calcined S-2M-150-200 prepared with the addition of HAc exhibits a (100) diffraction of much stronger intensity, further revealing that the addition of HAc is beneficial for the synthesis of highly ordered mesoporous materials. According to the XRD results shown above, it can be seen that by simultaneously adjusting hydrothermal treatment pH and adding HAc, highly ordered mesoporous materials can be successfully synthesized at a very high hydrothermal treatment temperature as high as 200 °C.

The N_2 adsorption−desorption isotherms and corresponding pore size distribution curves of the calcined

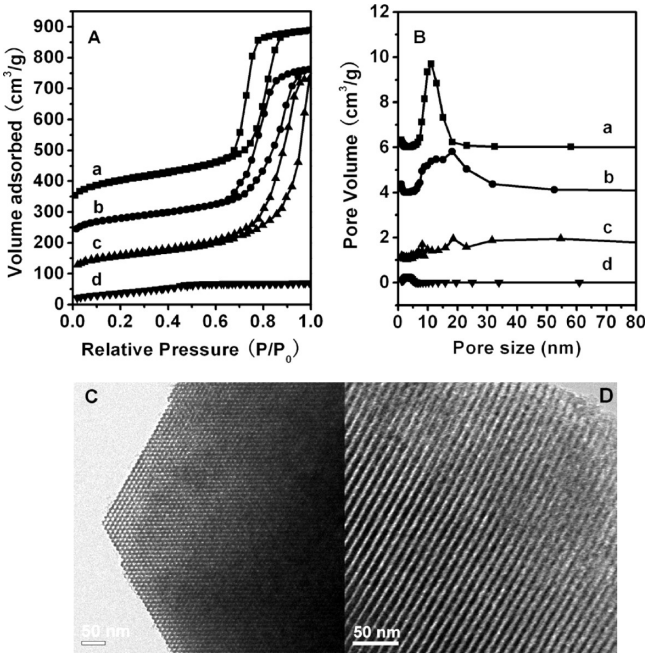

Figure 2. N_2 adsorption/desorption isotherms (A) and the pore size distribution curves (B) of calcained samples (a) S-1.65-150-200, (b) S-1.65-0-200, (c) S-2M-150-200, and (d) S-2M-0-200. TEM images (C and D) of calcined S-1.65-150-200 viewed along [100] and [110] directions, respectively. For clarity, in part A, the isotherms of S-1.65-150-200, S-1.65-0-200, and S-2M-150-200 are offset along the *Y*-axis by 300, 200, and 100 cm^3/g, respectively. In part B, the *Y*-axis value is 6, 4, and 1 cm^3/g higher for samples S-1.65-150-200, S-1.65-0-200, and S-2M-150-200, respectively.

samples are shown in Figure 2. Calcined S-1.65-150-200 prepared by simultaneously adjusting the hydrothermal treatment pH and adding HAc during synthesis exhibits a typical type IV isotherm and a very steep capillary condensation step occurring at a relative pressure (P/P_0) ranging from 0.70 to 0.85, characteristic of ordered mesoporous materials with large and uniform mesopores. Calcined S-1.65-150-200 has a BET surface area of 367 m^2/g, a pore volume of 0.91 cm^3/g, and an average pore size of 11.2 nm calculated from the adsorption branch using the Barrett−Joyner−Halenda (BJH) model (Table 1). However, for calcined samples S-1.65-0-200 and S-2M-150-200 prepared without adding HAc or adjusting pH, respectively, isotherms show a less steep capillary condensation step shifting toward higher P/P_0. It is noticeable that for calcined S-2M-0-200 prepared with neither adjusting pH nor adding HAc, the mesostructure has been essentially destroyed during the high temperature hydrothermal treatment process, and the porosity is very low as reflected from the isotherm of this sample (Figure 2A,d). The dimension and uniformity of mesopores in different materials are directly reflected by the pore size distribution curves. From Figure 2B, it can be clearly seen that calcined sample S-1.65-150-200 possesses the narrowest pore size distribution among all of the samples. In addition, by comparing the XRD patterns (curves b and c in Figure 1) and pore size distributions (curves b and c in Figure 2B) of S-1.65-0-200 and S-2M-150-200, it is clear that the influence of pH adjustment is more significant than HAc addition when a high temperature hydrothermal treatment process is employed in fabricating ordered mesoporous materials.

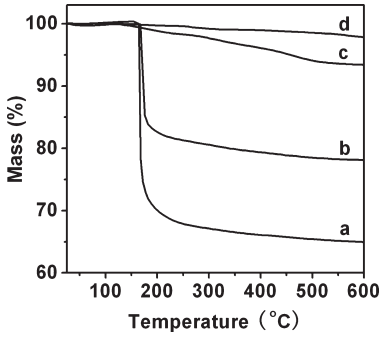

Figure 3. TG curves of as-synthesized (a) S-1.65-150-200, (b) S-1.65-0-200, (c) S-2M-150-200, and (d) S-2M-0-200.

The highly ordered mesostructure of calcined S-1.65-150-200 is further confirmed by TEM analysis. Figure 2C and D show highly ordered hexagonal arrays of mesopores with uniform pore size and wall thickness recorded along [100] and [110] directions, respectively. Judged from the white−dark contrast of TEM images, the distance between two neighboring mesochannels is ca. 11 nm, in good agreement with the value calculated from the XRD analysis (see curve a in Figure 1 and Table 1).

Figure 3 shows the TG curves of the four as-synthesized materials introduced in the previous section. For as-synthesized samples S-1.65-150-200 and S-1.65-0-200, there is only one main mass loss step in the temperature range from 150 to 250 °C, which is characteristic for the decomposition of polymeric surfactant P123 existing inside as-synthesized SBA-15 materials.[51−54] The mass loss percentages in the range of 150−600 °C for as-synthesized S-1.65-150-200, S-1.65-0-200, S-2M-150-200, and S-2M-0-200 are 35.1, 21.9, 6.6, and 2.2%, respectively, as summarized in Table 1. It is interesting to note that, for these four as-synthesized samples, the amount of the surfactant lost is directly related to the mesostructural regularity of the corresponding products. S-1.65-150-200 with the highest mesostructural ordering shows the largest mass loss percentage among four samples. Moreover, by comparing the mass loss percentages of S-1.65-0-200 and S-2M-150-200, it is shown that adjusting hydrothermal treatment pH (without adding HAc) is more advantageous in maintaining higher amount of P123 in as-synthesized material and thereby producing relatively ordered structure compared to only adding HAc (without adjusting pH) in the synthesis.

To elucidate the effect of pH during the high temperature hydrothermal treatment process on the resulting mesostructure, a series of samples S-*X*-150-200 were synthesized by adjusting the hydrothermal treatment

(51) Berube, F.; Kaliaguine, S. *Microporous Mesoporous Mater.* **2008**, *115*, 469.
(52) Mansur, C. R. E.; Gonzalez, G.; Lucas, E. F. *Polym. Degrad. Stab.* **2003**, *80*, 579.
(53) Coutinho, A.; Quintella, S. A.; Araujo, A. S.; Barros, J. M. F.; Pedrosa, A. M. G.; Fernandes, V. J.; Souza, M. J. B. *J. Therm. Anal. Calorim.* **2007**, *87*, 457.
(54) Kruk, M.; Jaroniec, M.; Ko, C. H.; Ryoo, R. *Chem. Mater.* **2000**, *12*, 1961.

pH while the other synthesis conditions remained exactly the same. The XRD patterns of calcined S-*X*-150-200 are shown in Figure 4. In the pH range of 1−3 (*X* = 1.26, 1.65, 2.63), the XRD patterns of the three samples show three well-resolved diffraction peaks that can be indexed to a highly ordered hexagonal mesostructure. When the hydrothermal treatment pH is 1.65, S-1.65-150-200 shows the XRD pattern with the highest peak intensity. However, when the hydrothermal treatment pH is either lower than 1 or higher than 3, the higher order (110 and 200) diffractions can not be observed in the XRD patterns of calcined materials (*X* = 0.42, 0.20, 0.16, 3.99, 4.66). Moreover, the intensity of the first diffraction peak also decreases significantly, indicating the decreased mesostructural ordering. It can be concluded that there exists an optimum hydrothermal treatment pH in the range from 1 to 3, at which highly ordered mesoporous materials can be successfully synthesized at a hydrothermal temperature of 200 °C.

Figure 5A shows the TG curves of as-synthesized samples S-*X*-150-200. It can be seen that the TG curves of as-synthesized samples S-*X*-150-200 can be divided into two groups according to the hydrothermal treatment pH. When the hydrothermal treatment pH is < 1, all of the samples exhibit two steps of mass loss, one in the temperature range of 150−250 °C, and the other in the higher temperature range of 250−350 °C. This phenomenon is the most distinctive for S-0.42-150-200. On the other hand, when the hydrothermal treatment pH is > 1, only one mass loss step in the temperature range of 150−250 °C can be observed in this group of samples.

Figure 5B displays the corresponding mass losses calculated from Figure 5A in the temperature range of 150−600 °C as a function of the hydrothermal treatment pH for as-synthesized S-*X*-150-200. For the first group of as-synthesized S-*X*-150-200 prepared at the hydrothermal treatment pH < 1 (*X* = 0.16, 0.20, 0.42), the mass loss percentage decreases rapidly with the decreasing pH. It is also noted that as-synthesized S-0.16-150-200 shows a small mass loss percentage of 5%, similar to that of S-2M-150-200 obtained under a high acidic condition.

To understand the pH-dependent mass loss behavior and the unusual two-stage mass loss profiles for this group of samples, first we need introduce our experimental observations. As shown in Figure 6, as-synthesized S-*X*-150-200 samples hydrothermally treated at pH > 1 (e.g., pH = 1.26) are all white powders (Figure 6a). However, the as-synthesized samples hydrothermally treated at pH < 1 are black, and some black oily droplets are also

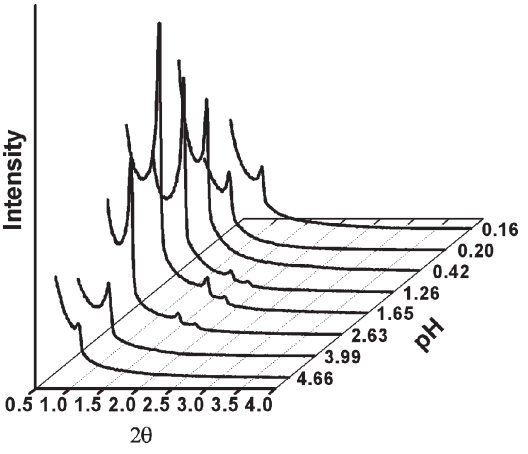

Figure 4. XRD patterns of calcined S-X-150-200.

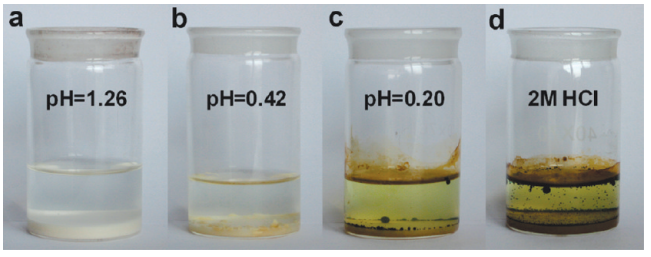

Figure 6. Digital camera images showing the samples after hydrothermal treatment at 200 °C and prepared under different conditions: (a) S-1.26-150-200, (b) S-0.42-150-200, (c) S-0.20-150-200, and (d) S-2M-0-200.

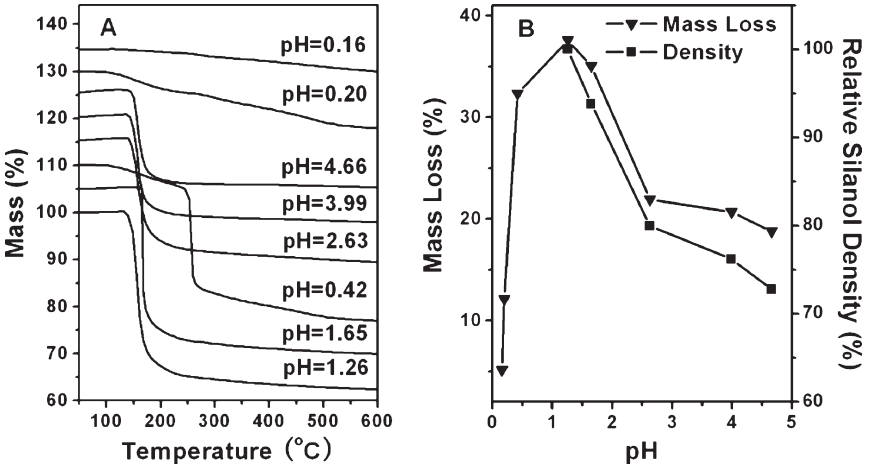

Figure 5. (A) TG curves of as-synthesized samples S-X-150-200. (B) Plot of the surfactant mass loss (%) and relative silanol density (%) as a function of hydrothermal treatment pH for S-X-150-200. For clarity, the TG curves of S-0.16-150-200, S-0.20-150-200, S-4.66-150-200, S-3.99-150-200, S-2.63-150-200, S-0.42-150-200, and S-1.65-150-200 are offset from 35%, 30%, 25%, 20%, 15%, 10%, and 5% along the *Y*-axis, respectively. The relative silanol densities were calculated from FTIR data, and the relative silanol density of the sample S-1.26-150-200 was considered as 100%.

observed in the suspension (Figure 6b and c). Moreover, the color of samples becomes blacker as pH decreases. Such observations are also demonstrated for other samples synthesized in our study. For example, S-2M-0-200 prepared under the strongest acidic condition shows the blackest color and the reaction mixture contains a large number of black oily droplets after the hydrothermal treatment at 200 °C (Figure 6d).

It should be noted that in our synthesis before the hydrothermal treatment, the white powders were filtrated and washed three times to remove the residue organics outside the pore channels. Therefore, the occurrence of the black samples as well as the black oily droplets after the high temperature (200 °C) hydrothermal treatment should be attributed to the partial oxidation of block copolymers embedded within the pores. It is well-known that the oxidation potential of oxygen increases as the acidity and temperature increase. Although such a potential is hard to calculate for a real high temperature hydrothermal treatment process, our experimental observations together with the TG results are consistent with the influence of pH upon the oxidation potential of oxygen. At a high hydrothermal treatment temperature of 200 °C, the pH value at approximately 1 is the turning point in our system. When pH is <1, the oxidation potential of oxygen is high enough to partially oxidize block copolymers into partially carbonized intermediates. Moreover, the extent of the block copolymer decomposition increases with the decreasing pH due to the increased oxidation potential of oxygen, which explains the mass loss−pH dependence at pH $<$ 1 (Figure 5) and the change in the color of as-synthesized samples (Figure 6). In addition, the two-step mass loss profiles observed for this group of samples can be explained. The first decomposition step occurring at 150−250 °C is attributed to partially remained block copolymers in the pore channels,[51−54] while the second step at 250−350 °C should be associated with the partially oxidized carbonized intermediates.

For the second group of samples hydrothermally treated under relatively weaker acidic conditions (pH $>$ 1), the much lower oxidation potential of oxygen cannot oxidize the organic template, leading to white color as-synthesized samples with only one step of major mass loss occurring at 150−250 °C, which can be attributed to the decomposition of the block copolymers. Interestingly, the mass loss percentages decrease as pH increases (Figure 5B), significantly different from the pH-dependent behavior for the first group samples. It is also notable that such a trend is analogous to the pH-dependent condensation profile of silica, where the condensation rate of silanols is the slowest at the isoelectric point of silica (pH $\sim$ 2).[55−58] We therefore hypothesize that the mass loss−pH dependence profile for the second group of samples (pH $>$ 1) should be closely associated with the pH-dependent condensation profile of silanols.

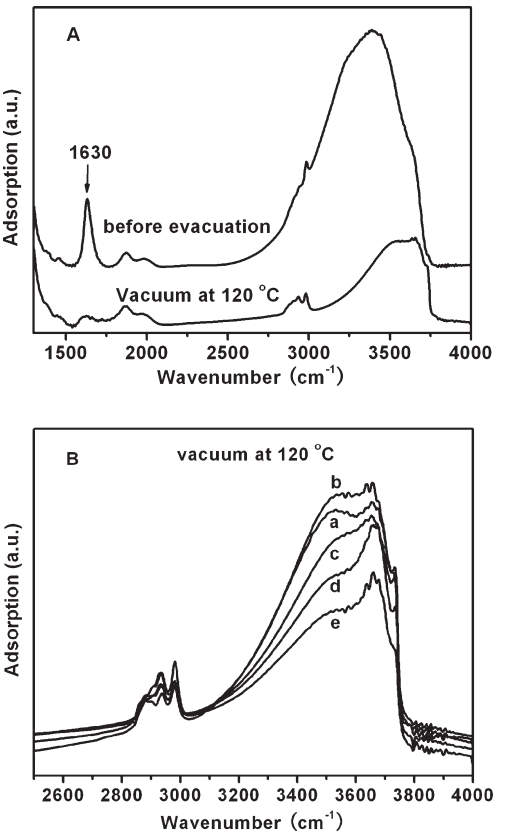

Figure 7. (A) FTIR spectra of surfactant extracted sample S-1.65-150-200 before and after evacuation under vacuum. (B) FTIR spectra of surfactant extracted samples S-X-150-200 after evacuation under vacuum: (a) S-1.26-150-200, (b) S-1.65-150-200, (c) S-2.63-150-200, (d) S-3.99-150-200, and (e) S-4.66-150-200.

To underpin our hypothesis, we use in situ FTIR to semiquantitatively compare the relative silanol density for the surfactant-extracted samples S-*X*-150-200 when the hydrothermal treatment pH is >1. The concentration of silanol groups is measured from the integral area of Si−OH band after the complete removal of physisorbed water (Figure 7). The relative silanol density is calculated from the concentration of silanols per surface area (S_{BET}) of materials (assuming that the relative silanol density of extracted S-1.26-150-200 is 100%), and the results are shown in Figure 5B. As it can be seen from Figure 7A, the FTIR spectrum of surfactant-extracted sample S-1.65-150-200 before evacuation under vacuum shows one sharp band at 1630 cm^{-1}, which can be assigned to the bending mode of physisorbed water molecules.[59] The broad adsorption at 2800−3800 cm^{-1} is mainly attributed to the stretching OH (νO−H) contributed by both water and silanols. However, after evacuation under vacuum, the band arising from the bending mode of water (1630 cm^{-1}) cannot be detected from the FTIR spectrum (Figure 7A), indicating that the physisorbed water has been mostly removed and the νO−H band can now be used to calculate the concentration of silanol groups.

(55) Hench, L. L.; West, J. K. *Chem. Rev.* **1990**, *90*, 33.
(56) Cihlar, J. *Colloid Surf. A-Physicochem. Eng. Asp.* **1993**, *70*, 253.
(57) Coltrain, B. K.; Kelts, L. W. *The Chemistry Of Hydrolysis And Condensation Of Silica Sol-Gel Precursors: Colloid Chemistry Of Silica*; American Chemical Society: Washington, DC, 1994; p 403.
(58) Boissiere, C.; Larbot, A.; Bourgaux, C.; Prouzet, E.; Bunton, C. A. *Chem. Mater.* **2001**, *13*, 3580.
(59) Blin, J. L.; Carteret, C. *J. Phys. Chem. C* **2007**, *111*, 14380.

Scheme 1. Proposed Mechanism Schematically Showing the Influence of Hydrothermal Treatment (HT) pH on the Final Composite Mesostructure

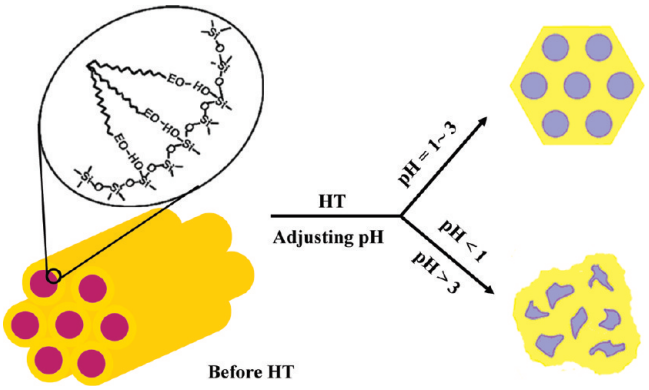

Figure 7B shows the FTIR spectra of surfactant-extracted S-*X*-150-200 samples with the hydrothermal treatment pH > 1. The bands detected at 2912, 2949, and 2986 cm^{-1} are assigned to the stretching vibrations of CH groups of the surfactant, suggesting that, even after three times of ethanol extraction, the block copolymer surfactants cannot be completely removed.[54,59−61] These bands, however, do not overlap with the νSiO−H band observed at 3100−3750 cm^{-1}. As shown in Figure 7B, generally increasing the hydrothermal treatment pH decreases the silanol concentration of the surfactant-extracted S-*X*-150-200 samples as judged from the integral area of νO−H band. Nevertheless, the silanol concentration of S-1.65-150-200 is a little higher than that of S-1.26-150-200. In mesoporous silica, it is reported that above 95% of silanol groups are surface silanols.[59] To take the influence of surface area into account, we further employ the N_2 adsorption method to determine the surface area of the surfactant-extracted samples and then compare the relative silanol densities of samples hydrothermally treated at different pH values. As shown in Figure 5B, the relative silanol density−pH dependence matches perfectly with the mass loss−pH dependence as discussed above. This observation strongly suggests an inherent correlation between the surfactant mass loss and silanol density, which is a bridge to understand the relationship between mesostructural ordering and hydrothermal treatment pH.

The influence of hydrothermal treatment pH on mesostructure regularity after a high temperature hydrothermal treatment process is schematically shown in Scheme 1. Before the hydrothermal treatment, the ordered mesostructure has already formed in SBA-15 type materials despite the partially condensed silica walls.[62−65] During the further high temperature hydrothermal treatment process, the composite mesostructure, i.e., ordered arrays of micelles (such as cylindrical micelles in our material) embedded within silica matrices, experiences further silica wall condensation and framework shrinkage. The preservation of surfactant micelles within the pore channels is therefore important to support the silica framework and maintain the ordered mesostructure during the high temperature hydrothermal treatment process. On the other hand, if the surfactant micelles have been partially or completely removed from the pore channels during the hydrothermal treatment process, the silica framework will lose the support during the further condensation and framework shrinkage, thus the mesostructure will partially or completely collapse.

The hydrogen-bonding interactions[66] between silanols and the EO moiety of the block copolymer surfactants at the inorganic/organic interface (Scheme 1) is the key to further understand the influence of hydrothermal treatment pH on the final mesostructure. Increasing the density of silanol located at the pore wall surface can enhance the hydrogen-bonding and entrap block copolymer micelles within the pores. When the hydrothermal treatment pH is near the isoelectric point of silica, the further condensation of silica during the hydrothermal treatment is the slowest,[55−58] therefore leading to silica walls with the highest silanol concentration. Consequently, the surfactant micelles are entrapped in the pores with the largest amount (reflected by the TG mass loss percentage), resulting in highly ordered mesostructured materials (e.g., S-1.26-150-200 and S-1.65-150-200). When the hydrothermal treatment pH is increased, the further condensed silica wall and decreased silanol density may retain less block copolymers, leading to mesostructured materials with decreased structural regularity. As shown in Scheme 1, the ordered hexagonal mesostructure cannot be obtained when the hydrothermal treatment pH is higher than 3. On the other end, when the hydrothermal treatment pH is lower than 1, ordered mesoporous materials can neither be synthesized due to the loss of surfactant micelles originally filled in the pores. However, the underlying reason in this regime should be attributed to the oxidation of organic surfactants under the conditions of increased acidity and high temperature. Therefore, we conclude that when a high temperature (200 °C) hydrothermal treatment is employed, ordered mesoporous materials can only be obtained in a hydrothermal treatment pH range of 1−3.

To further support the above mechanism, the interaction between silanol groups and P123 micelles was validated by a P123 readsorption experiment of the surfactant-removed samples (S-2M-0-100) by both the calcination and ethanol extraction methods (shown in Figure 8). It has been reported that there are much more silanol groups existing on the mesoporous walls of the

(60) Xiao, L. P.; Li, J. Y.; Jin, H. X.; Xu, R. R. *Microporous Mesoporous Mater.* **2006**, *96*, 413.
(61) Bae, Y. K.; Han, O. H. *Microporous Mesoporous Mater.* **2007**, *106*, 304.
(62) Ruthstein, S.; Schmidt, J.; Kesselman, E.; Talmon, Y.; Goldfarb, D. *J. Am. Chem. Soc.* **2006**, *128*, 3366.
(63) Ruthstein, S.; Schmidt, J.; Kesselman, E.; Popovitz-Biro, R.; Omer, L.; Frydman, V.; Talmon, Y.; Goldfarb, D. *Chem. Mater.* **2008**, *20*, 2779.
(64) Ruthstein, S.; Frydman, V.; Kababya, S.; Landau, M.; Goldfarb, D. *J. Phys. Chem. B* **2003**, *107*, 1739.
(65) Hsu, Y. C.; Hsu, Y. T.; Hsu, H. Y.; Yang, C. M. *Chem. Mater.* **2007**, *19*, 1120.
(66) Bagshaw, S. A.; Prouzet, E.; Pinnavaia, T. J. *Science* **1995**, *269*, 1242.

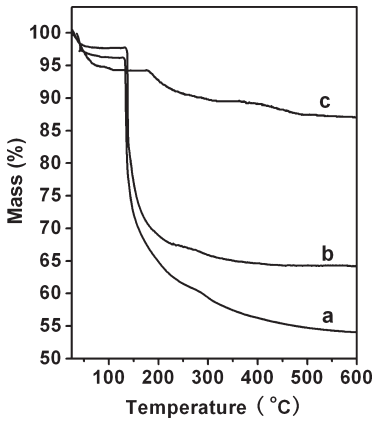

Figure 8. TGA curves of (a) surfactant extracted S-2M-0-100 with readsorbed P123, (b) calcined S-2M-0-100 with readsorbed P123, and (c) surfactant extracted S-2M-0-100 without readsorbed P123.

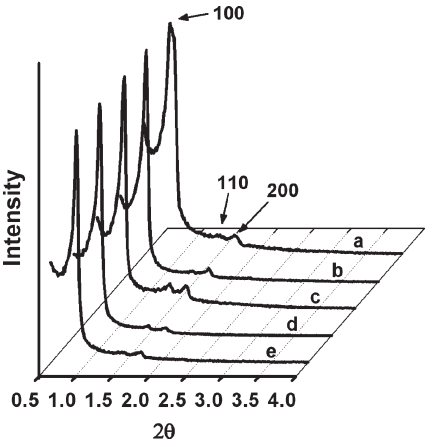

Figure 9. XRD patterns of as-synthesized samples S-2M-Y-100 prepared with different n_{HAc}/n_{P123} and hydrothermally treated by 2 M HCl at 100 °C: (a) S-2M-0-100, (b) S-2M-50-100, (c) S-2M-150-100, (d) S-2M-300-100, and (e) S-2M-400-100.

surfactant-removed mesoporous materials by extraction than on those of calcined samples.[61,67] To take into consideration the mass loss of water during further condensation of silanols and partially retained P123 in extracted S-2M-0-100 (as shown in Figure 7B), the TGA of surfactant-extracted S-2M-0-100 without P123 adsorption was also measured (Figure 8). From the TGA profiles, it can be calculated that the surfactant-extracted and calcined S-2M-0-100 can readsorb 40.2% and 33.0% (mass percentage) P123 molecules, respectively. The surfactant-extracted and calcined S-2M-0-100 have surface areas of 407 and 577 m^2/g and pore volumes of 0.71 and 0.83 cm^3/g, respectively. Despite its relatively smaller surface area and pore volume, the surfactant-extracted sample can adsorb 1.3 times more P123 compared to the calcined sample, indicating that the higher silanol density in the former material accounts for the larger amount of P123 readsorption. This observation is another support to our proposed mechanism: there exists hydrogen bonding between silanols and P123 molecules; increasing the silanol density will enhance the interaction and favor the entrapment of surfactants within the pore channels, which is helpful to synthesize highly ordered mesoporous materials.

To understand the role of HAc and choose an optimum amount of HAc to synthesize highly ordered mesoporous materials, we synthesized a series of S-2M-*Y*-100 via the traditional route (hydrothermally treated with 2.0 M HCl at 100 °C)[14,15] in the presence of different amount of HAc (Y = 0, 50, 150, 300, 400). Here, it should be pointed out that because P123 in a strong acidic medium decomposes at 200 °C, thus we use a hydrothermal treatment temperature of 100 °C in the synthesis of this group of samples. Figure 9 shows the XRD patterns of as-synthesized S-2M-*Y*-100. Three diffraction peaks can be observed for all of the samples, however, the FWHMs calculated from the (100) diffractions are 0.19, 0.13, 0.10, 0.12, and 0.12° for the samples obtained at Y = 0, 50, 150, 300, 400, respectively. As-synthesized sample S-2M-150-100 exhibits not only the narrowest (100) diffraction, but also the most clearly resolved higher angle (110 and 200) diffractions, demonstrating that the addition of HAc can increase the mesostructural ordering and there exists an optimum HAc amount (Y = 150).

It is well-known that HAc can behave as a ligand and bond with silicon atoms of silicon alkoxides in a bidentate or bridging fashion, which slows down the hydrolysis−condensation reaction of silicon alkoxides in solution.[68−70] As a result, the addition of HAc in the synthesis can produce more silanol groups on the silica walls that interact with P123 micelles by hydrogen bonding (Scheme 1) and thus minimize the loss of P123 during further hydrothermal treatment process, leading to improved mesostructural regularity. This is further supported by the comparison between S-2M-150-200 and S-2M-0-200 (see Figures 1−3). When the other synthesis conditions are exactly the same, the addition of HAc can increase the amount of P123 retained in the as-synthesized samples (Figure 3) and lead to a certain degree of improvement in mesostructural ordering. However, further increasing HAc amount may affect the cooperative self-assembly between P123 and HAc coordinated siliceous species, leading to a slightly decreased structural regularity. We therefore take Y = 150 as an optimum point to synthesize highly ordered mesoporous materials in our approach.

To investigate the influence of hydrothermal treatment temperature on the structure of resultant mesoporous materials, we synthesized a group of S-1.65-150-*T* samples at different hydrothermal treatment temperatures (T = 160, 180, 200, 220 °C) when the hydrothermal treatment pH is 1.65 and the n_{HAc}/n_{P123} is 150. From the powder XRD patterns of calcined S-1.65-150-*T* samples (Figure 10), it can be seen that all S-1.65-150-*T* samples possess a highly ordered hexagonal mesostructure. Even

(67) van Grieken, R.; Calleja, G.; Stucky, G. D.; Melero, J. A.; Garcia, R. A.; Iglesias, J. *Langmuir* **2003**, *19*, 3966.
(68) Tsai, M. T. *J. Non-Cryst. Solids* **2002**, *298*, 116.
(69) Tsung, C. K.; Fan, J.; Zheng, N. F.; Shi, Q. H.; Forman, A. J.; Wang, J. F.; Stucky, G. D. *Angew. Chem.-Int. Ed.* **2008**, *47*, 8682.
(70) Fan, J.; Boettcher, S. W.; Stucky, G. D. *Chem. Mater.* **2006**, *18*, 6391.

for the sample S-1.65-150-220, three well-resolved diffractions can still be clearly observed. With increasing hydrothermal treatment temperature from 160 to 220 °C, the first diffraction peaks of calcined S-1.65-150-*T* samples are shifted toward higher angles, suggesting that the unit cell (*a*) parameter is decreased from 11.2 to 10.2 nm (Table 2). This observation can be attributed to the occurrence of the silica framework shrinkage at higher hydrothermal treatment temperatures.

The N_2 adsorption−desorption isotherms and the corresponding pore diameter distribution curves of calcined S-1.65-150-*T* samples are shown in Figure 11. All calcined S-1.65-150-*T* samples display typical type IV curves and an H1-type hysteresis loop. As summarized in Table 2, the pore sizes and pore volumes of S-1.65-150-*T* samples systematically increase with the hydrothermal treatment temperature. However, the capillary condensation step of calcined S-1.65-150-220 is less steep compared to the other three samples. As a consequence, S-1.65-150-220 shows a relatively broader pore size distribution curve compared to S-1.65-150-*T* samples hydrothermally treated at lower temperatures (T = 160, 180, 200 °C). Therefore, in order to synthesize highly ordered mesoporous materials with condensed silica walls, we choose a hydrothermal treatment temperature of 200 °C during our previous experiments.

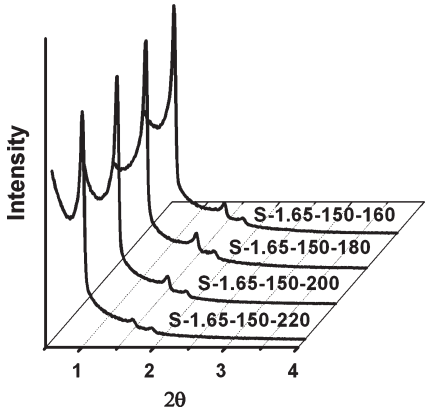

Figure 10. XRD patterns of calcined S-1.65-150-*T*.

Hydrothermal Stability

The aim of high temperature hydrothermal treatment of mesoporous materials is to increase the condensation degree of silica walls, consequently, to increase the hydrothermal stability of mesoporous materials. Therefore, the ^{29}Si MAS NMR spectrum is employed to provide direct evidence of silica cross-linking of mesostructured materials synthesized by our method (Figure 12). The ^{29}Si NMR spectrum of as-synthesized S-1.65-150-200 shows primarily fully condensed Q^4 silica units ($\delta = -112$ ppm) together with a small contribution from incompletely cross-linked Q^3 ($\delta = -102$ ppm) and Q^2 ($\delta = -92$ ppm). After deconvolution, the ratio of $Q^4/(Q^3 + Q^2)$ calculated is 3.4. This $Q^4/(Q^3 + Q^2)$ ratio is much higher than that (1.5) of S-2M-0-100 prepared via the traditional route (Figure 12B).[14,15] We also measured the ^{29}Si MAS NMR spectrum of calcined S-1.65-150-200 (Figure 12C), in which the Q^3 peak decreases remarkably, indicating that the degree of silica cross-linking has been increased after calcination. The ratio of Q^4/Q^3 after deconvolution is calculated to be 6.7 for calcined S-1.65-150-200.

Figure 1S (of the Supporting Information) shows the XRD patterns and N_2 adsorption−desorption isotherms of calcined S-2M-0-100 and S-1.65-150-200 after being treated in boiling water for 168 h. For two samples, the (100), (110), and (200) reflections can be clearly observed (Figure 1S, A), indicating that the highly ordered mesostructures were still kept. Moreover, the cell parameter

Table 2. Physicochemical Properties of Calcined S-1.65-150-*T* Prepared at Different Hydrothermal Treatment Temperatures[a]

sample	*a* (nm)	D_p (nm)	S_{BET} (m^2/g)	V_p (cm^3/g)
S-1.65-150-160	11.2	9.8	397	0.80
S-1.65-150-180	10.7	11.1	390	0.82
S-1.65-150-200	10.4	11.2	367	0.91
S-1.65-150-220	10.2	11.2	391	1.03

[a] a = cell dimension; D_p = pore diameter; V_p = total pore volume.

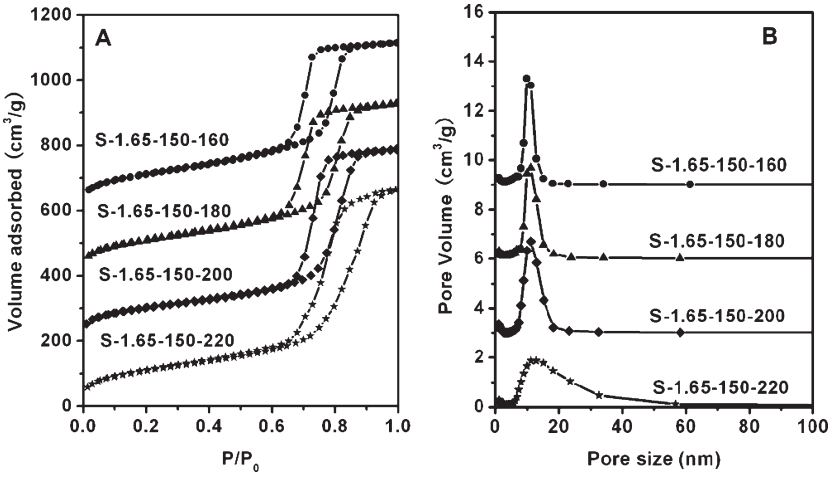

Figure 11. N_2 adsorption/desorption isotherms (A) and the pore size distribution curves (B) of calcained S-1.65-150-*T*. For clarity, in part A, the isotherms of S-1.65-150-160, S-1.65-150-180, and S-1.65-150-200 are offset along the *Y*-axis by 600, 400, and 200 cm^3/g, respectively. In part B, the *Y*-axis value is 9, 6, and 3 cm^3/g higher for sample S-1.65-150-160, S-1.65-150-180, and S-1.65-150-200, respectively.

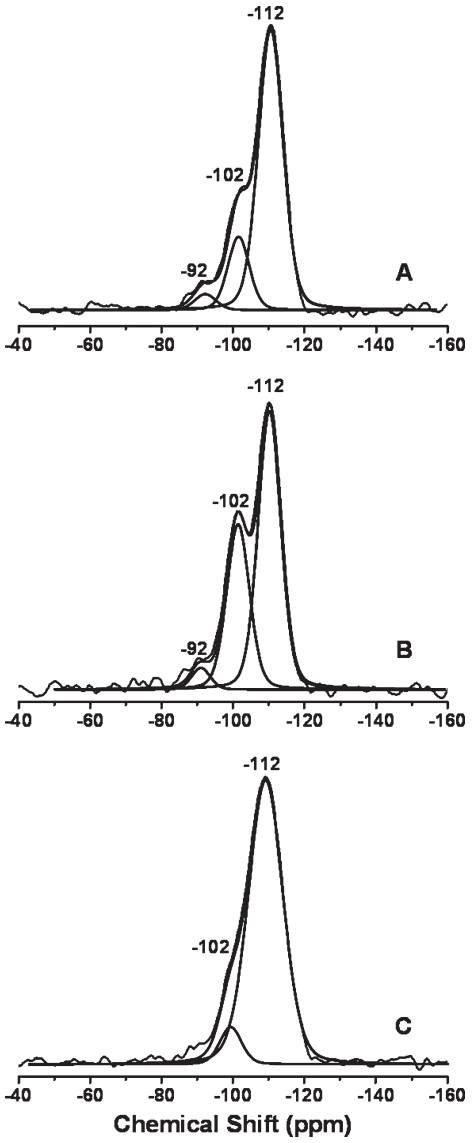

Figure 12. ^{29}Si NMR spectra of as-synthesized (A) S-1.65-150-200, (B) S-2M-0-100, and (C) calcined S-1.65-150-200.

does not change for S-1.65-150-200 after test (Table 1S). S-2M-0-100 and S-1.65-150-200 after treatment in boiling water for 168 h still exhibit type IV isotherms with a very steep capillary condensation step, characteristic of ordered mesoporous materials with uniform mesopores (Figure 1S, B). From Table 1S, it can be seen that the treated S-1.65-150-200 retained 87.5% of the specific surface area and 98.7% of the pore volume compared to the untreated sample, which is better than that of S-2M-0-100 prepared with the traditional method reported by Zhao and co-workers.[14,15]

Compared to the treatment in boiling water (100 °C), the steam treatment at 800 °C is a much higher standard and much more rigorous testing method (also the industry application standard) to evaluate the hydrothermal stability. Take the mesoporous aluminosilicates prepared by a combination of postsynthesis grafting and hydrothermal treatment[27] for example, although the samples exhibited high hydrothermal stability in boiling water, the mesostructure could not be well maintained after steam

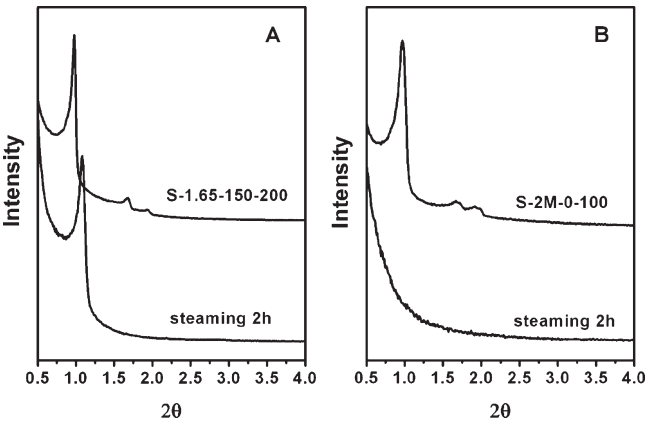

Figure 13. XRD patterns of calcined (A) S-1.65-150-200 and (B) S-2M-0-100 steamed at 800 °C for 2 h.

treatment at 800 °C.[37,38] Figure 13A gives the XRD patterns of calcined S-1.65-150-200 before and after steam treatment at 800 °C for 2 h. It can be seen that S-1.65-150-200 still shows a very strong (100) diffraction after steam treatment; however, the higher angle (110 and 200) diffractions cannot be observed. The cell parameter decreases to 9.4 nm due to the further framework shrinkage during the high temperature steam treatment process. In contrast, for S-2M-0-100 prepared by the traditional method at 100 °C without the addition of HAc, no diffraction peak can be observed after the steam treatment (Figure 13B), indicating that the mesostructure of S-2M-0-100 has been destroyed. This conclusion is further confirmed by the N_2 adsoption−desorption measurements (Figure 14). For S-1.65-150-200 after steam treatment at 800 °C for 2 h, its N_2 adsoption−desorption curve still maintains a typical IV isotherm with an H1-type hysteresis loop (Figure 14A), and the pore size distribution curve (Figure 14B) is as narrow as that of untreated S-1.65-150-200 (Figure 2B), indicating that the hexagonal mesostructure is well-preserved. As presented in Table 3, the steamed S-1.65-150-200 retains 75.2% of the specific surface area and 52.7% of the pore volume compared to the untreated sample, higher than those of the steamed samples prepared with the fluororcarbon-hydrocarbon surfactant mixtures as templates.[20,47] In contrast, the steamed S-2M-0-100 shows an unobvious hysteresis loop and an indiscernible pore size distribution (Figures 14), indicating that the mesostructure is completely destroyed (see also Table 3). It is worthy of noting that the mean pore size calculated from the adsorption branch of calcined S-1.65-150-200 is even larger than the cell parameter, which is due to the formation of disordered meso-tunnels on the silica walls during the high temperature hydrothermal treatment process.[71,72] The channel−channel communication through the meso-tunnels should facilitate diffusion and transport of molecules.

In order to further increase the hydrothermal stability of mesoporous materials, we synthesized alumina

(71) Fan, J.; Yu, C. Z.; Wang, L. M.; Tu, B.; Zhao, D. Y.; Sakamoto, Y.; Terasaki, O. *J. Am. Chem. Soc.* **2001**, *123*, 12113.
(72) Galarneau, A.; Cambon, N.; Di Renzo, F.; Ryoo, R.; Choi, M.; Fajula, F. *New J. Chem.* **2003**, *27*, 73.

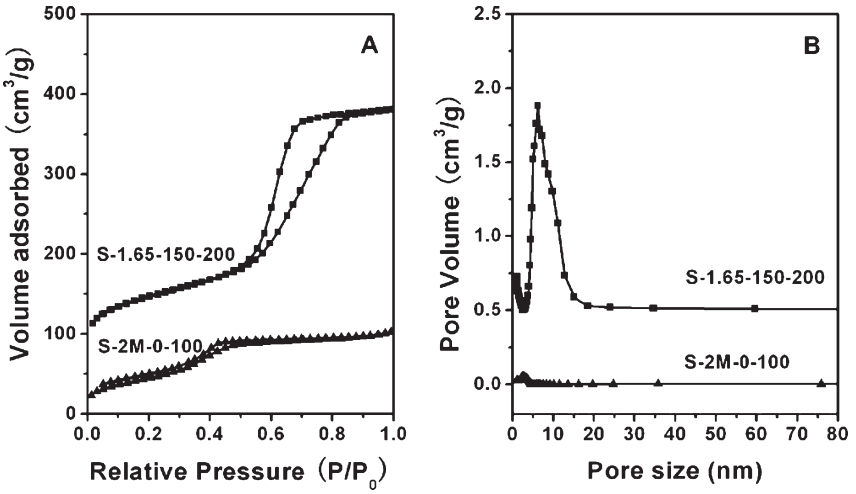

Figure 14. N_2 isotherms (A) and the corresponding pore size distribution curves (B) of S-1.65-150-200 and S-2M-0-100 steamed at 800 °C for 2 h. For clarity, in part A, the isotherm of S-1.65-150-200 is offset along the *Y*-axis by 70 cm^3/g. In part B, the *Y*-axis value is 0.5 cm^3/g higher for sample S-1.65-150-200.

Table 3. Structure Parameters of the Samples Calcined at 650 °C and Steamed at 800 °C for 2 or 5 h[a]

sample	*a* (nm)	D_p (nm)	S_{BET} (m^2/g)	V_p (cm^3/g)	S_{BET} reduced (%)
S-1.65-150-200	10.4	11.2	367	0.91	
steaming 2 h	9.4	6.3	276	0.48	24.8
S-2M-0-100	10.5	8.0	577	0.83	
steaming 2 h			31	0.02	94.6
Al/S-1.65-150-200	10.7	11.2	371	0.90	
steaming 2 h	10.1	9.9	355	0.85	4.3
steaming 5 h	10.1	9.9	353	0.85	4.9

[a] *a* = cell dimension; D_p = pore diameter; V_p = total pore volume. Because S-2M-0-100 was rendered amorphous after the steam treatment, there is no *a* value and pore sizes for the steamed sample given in this table.

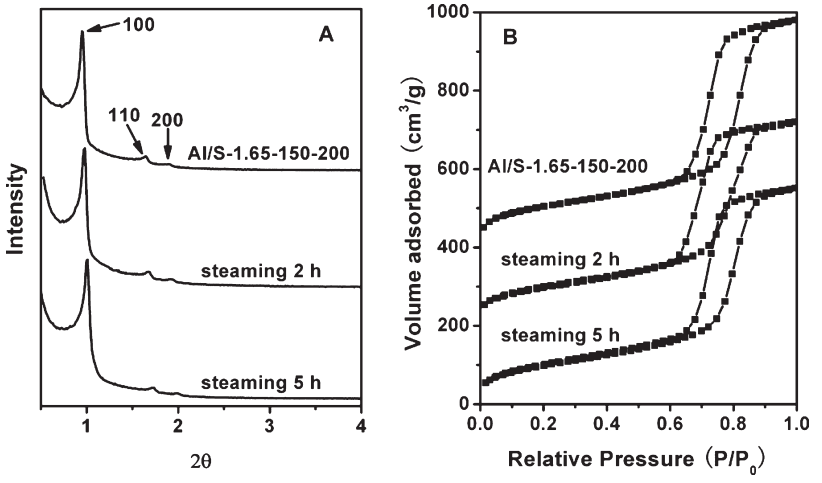

Figure 15. XRD patterns (A) and the N_2 isotherms (B) of calcined sample Al/S-1.65-150-200 steamed at 800 °C for 2 and 5 h. For clarity, in part B, the isotherms of Al/S-1.65-150-200 and steaming 2 h are offset along the *Y*-axis by 400 and 200 cm^3/g, respectively.

incorporated Al/S-1.65-150-200 through our approach with an initial Si/Al ratio of 30. The incorporation of Al could create Si−O−Al bonds, which are more resistant to attack from water, thus the incorporation of Al can effectively protect the framework against destruction during hydrothermal treatment.[25] Figure 15 shows XRD patterns and N_2 adsorption−desorption isotherms of Al/S-1.65-150-200 before and after being treated with steam at 800 °C for 2 and 5 h. It is shown that calcined Al/S-1.65-150-200 has a highly ordered hexagonal mesostructure (Figure 15A). After the steam treatment for 2 or 5 h, Al/S-1.65-150-200 still displays three well-resolved peaks, which can be indexed as the (100), (110), and (200) diffractions of a highly ordered hexagonal symmetry. Moreover, little change can be observed in the N_2 adsorption−desorption isotherms for Al/S-1.65-150-200 before and after the steam treatment (Figure 15B). From Table 3, the decreases in BET surface area and total pore volume after steam treatment at 800 °C for 2 h were 4.3% and 5.6%, respectively. Even after steam treatment at 800 °C for 5 h, the decreases in BET surface area and total pore volume were 4.9% and 5.6%, respectively. For

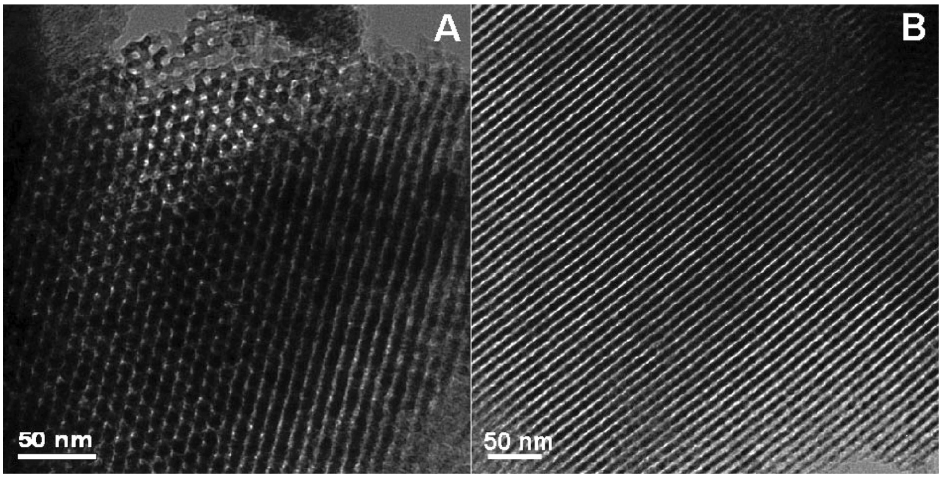

Figure 16. TEM images of Al/S-1.65-150-200 steamed at 800 °C for 2 h viewed along [100] and [110] directions, respectively.

comparison, the sample 1.5%Al-MUS-S prepared by using preformed zeolite seeds as precursors exhibited more decreases in BET surface area and total pore volume after steam treatment at 800 °C for 5 h, which were 21.3% and 56.6%, respectively.[37]

The well-ordered hexagonal arrays along [100] and [110] directions can also be seen from TEM images displayed in Figure 16A and B, respectively, showing a highly ordered 2D hexagonal pore ordering. All of these results indicate that Al/S-1.65-150-200 prepared by our method exhibits highly hydrothermal stability and highly ordered mesostructure even after being steamed at 800 °C for 2 and 5 h.

In our study, because the synthesis of Al/S-1.65-150-200 was carried out at a strong acidic condition (2 M HCl) following the original synthesis method[14,15] for a reasonable comparison, there is only a very small amount of Al incorporated into the product. Compared with the initial Si/Al ratio of 30 during the synthesis, the energy dispersive X-ray (EDX) and inductively coupled plasma (ICP) analyses show that the final Si/Al ratio of the calcined sample are 146 and 221, respectively, indicating that most of the Al species were not incorporated into the framework. After steam treatment at 800 °C for 5 h, the value of Si/Al ratio should be much increased, because the Al content can not be accurately measured by EDX, indicating that the high temperature steam treatment process may lead to dealuminization from the mesoporous framework.

Conclusion

We have developed a facile approach to synthesize highly ordered and highly hydrothermally stable mesoporous materials, which is built on the new understanding that the hydrothermal treatment process plays an important role in the synthesis of mesoporous materials. We have demonstrated that in order to use high temperature hydrothermal treatment to increase the inorganic framework cross-linking, an important precondition is that the organic surfactants must be retained as much as possible to maintain the preformed organic−inorganic composite mesostructure against framework shrinkage during hydrothermal treatment process. This requirement can be simply achieved by enhancing the surfactant−silanol interaction at the organic−inorganic interface through adjusting the hydrothermal treatment pH and adding acetic acid (HAc) during the synthesis. Moreover, the disadvantage of the hydrothermal treatment under strong acidic condition widely adopted in literatures has been revealed. Compared to previous reports,[20,46,47] our approach does not involve environmentally unfriendly or expensive agents such as additives of fluoride and fluorocarbon surfactants and, thus, is easy to scale up for industrial applications. Most strikingly, the highly ordered mesostructure of aluminosilicates synthesized by our approach can be maintained after steam treatment at 800 °C for 5 h with only a 4.9% decrease in their BET surface area. Our achievements add new contributions to understanding the hydrothermal process of synthesizing highly ordered mesoporous materials with highly hydrothermal stability. Clearly, this route is a potential method to be applied in industrialized manufacturing of highly ordered mesoporous silica and aluminosilicate materials with satisfactory hydrothermal stability, which have wide applications in the petroleum and petrochemical industry.

Acknowledgment. This work was financially supported by the State Key Research Program (Grant Nos. 2010CB226901 and 2006CB932302), the NSF of China (20721063 and 20825621), Shanghai STC (08DZ2270500, 07QH14003), SLADP (B108, B113), the Ministry of Education of China (20060246010), and FANEDD (200423).

Supporting Information Available: XRD patterns, adsorption isotherms, and the structure parameters of the samples calcined at 650 °C and hydrothermally treated in boiling water for 168 h. This material is available free of charge via the Internet at http://pubs.acs.org/.